Photoelectron spectroscopy of selenium- and tellurium-containing negative ions: SeO2-, Se2-, and Te2-

J. T. Snodgrass, J. V. Coe, K. M. McHugh, C. B. Freidhoff, and K. H. Bowen

J. Phys. Chem., **1989**, 93 (4), 1249-1254• DOI: 10.1021/j100341a016 • Publication Date (Web): 01 May 2002

Photoelectron Spectroscopy of Selenium- and Tellurium-Containing Negative Ions: SeO_2^-, Se_2^-, and Te_2^-

J. T. Snodgrass, J. V. Coe, K. M. McHugh, C. B. Freidhoff, and K. H. Bowen*

Department of Chemistry, The Johns Hopkins University, Baltimore, Maryland 21218
(Received: March 29, 1988)

We have measured the adiabatic electron affinities (EA's) of SeO_2, Se_2, and Te_2 and have determined limiting values for the electron affinities of TeO_2, Se_3, and Te_3 by applying the technique of negative ion photoelectron (photodetachment) spectroscopy to their negative ions. We found $EA(SeO_2) = 1.823 \pm 0.050$ eV, $EA(Se_2) = 1.94 \pm 0.07$ eV, $EA(Te_2) = 1.92 \pm 0.07$ eV, $EA(TeO_2) > 2.2$ eV, $EA(Se_3) > 2.2$ eV, and $EA(Te_3) \leq 2.7$ eV. By combining these values with thermochemical data available in the literature, we have calculated several previously unknown negative ion heats of formation and bond dissociation energies. Systematic variations in the electron affinities of small molecules containing group VIB atoms are also discussed. In addition, Te_3^- was found to have a propensity to photodissociate when irradiated with 2.540-eV photons.

Introduction

The group VIB elements exhibit extraordinarily rich chemistries, forming a diversity of molecules of broad chemical interest. In descending the VIB column of the periodic table, the elements show widely varying and increasingly metallic properties. In the past, the electron affinities of almost all of the atoms, of many simple oxygen- and sulfur-containing molecules, and of a few selenium- and tellurium-containing molecules have been determined by photodetachment and by other techniques.[1-6] Recently, we have measured the electron affinities of SeO, TeO, and TeH by conducting photodetachment studies on their negative ions,[7-9] using the technique of negative ion photoelectron spectroscopy.[10,11] Here, we report the results of our studies on SeO_2^-, Se_2^-, Te_2^-, TeO_2^-, Se_3^-, and Te_3^-, which provide adiabatic electron affinity values for SeO_2, Se_2, and Te_2 and limiting values for the electron affinities of TeO_2, Se_3, and Te_3. We also summarize all of our work to date on the electron affinities of selenium- and tellurium-containing molecules and examine systematic variations in the electron affinities of small molecules containing group VIB atoms.

Experimental Section

Negative ion photoelectron spectroscopy is conducted by crossing a mass-selected beam of negative ions with a fixed-frequency photon beam while energy analyzing the resulting photodetached electrons. The photoelectron spectrometer used in these experiments has been described in detail previously.[7] Briefly, negative ions are extracted from an ion source, accelerated to 500 eV, and mass analyzed by an $\vec{E} \times \vec{B}$ (Wien) velocity filter. The mass-selected ion beam then intersects a visible photon beam generated by an argon ion laser operating intracavity on a single line, $\lambda_0 = 488$ nm. For all results reported here, the photon energy was 2.540 eV. The kinetic energies of the photodetached electrons are determined by using a magnetically shielded hemispherical electron energy analyzer with a resolution of approximately 30 meV (fwhm).

Subtraction of the center-of-mass electron kinetic energy of an observed spectral feature from the fixed photon energy gives the transition energy, A, from an occupied level of the negative ion to an energetically accessible level of its corresponding neutral. In order to determine transition energies, the photoelectron spectrum of a calibrating ion of accurately known electron affinity is recorded immediately before and after the spectrum of the ion under study. The transition energy is then calculated via

$$A = EA_{cal} + \gamma(\Omega_{cal} - \Omega) + mW[(1/M_{cal}) - (1/M)] \quad (1)$$

where EA_{cal} is the electron affinity of the calibrant ion, γ is the electron kinetic energy scale compression factor (usually ~ 1.00), Ω is the laboratory kinetic energy peak position for the ion under study, Ω_{cal} is the laboratory kinetic energy of the electron affinity determining transition of the calibrating ion, m is the electron mass, W is the ion beam energy, and M_{cal} and M respectively are the masses of the calibrating ion and the ion under study.

Two different ion sources were used to generate the negative ions studied in these experiments. The ions SeO_2^-, Se_2^-, Se_3^-, and TeO_2^- were produced in a magnetically confined, hot-cathode discharge ion source which had been modified for high-temperature operation. Elemental selenium or tellurium was heated to temperatures that produced vapor pressure of ~ 1 Torr. A partial pressure of ~ 300 mTorr of N_2O gas was then admitted to the ion source, and a 2-20-mA electrical discharge was struck and maintained. The negative ion mass spectrum presented in Figure 1 shows the ions produced when selenium was used. The Te_2^- and Te_3^- ions were produced in a cold-cathode Penning discharge source. This source consists of a cylindrical anode, two disk cathodes located near opposite ends of the anode, an oven for supplying vapors to the anode, and an electromagnet for generating a magnetic field along the axis of the anode cylinder. Negative ions were extracted radially through an aperture in the side of the anode into the photoelectron spectrometer. To generate tellurium-containing negative ions, elemental tellurium was heated in the oven to ~ 500 °C to provide ~ 1 Torr of vapor pressure to the anode, and argon was added as the discharge support gas. A mass spectrum of the negative ions produced in this fashion showing the ions $Te_{n=1-7}^-$ is presented in Figure 2.

Results and Analysis

SeO_2^- and TeO_2^-. SeO_2^- and TeO_2^- are chemically analogous to SO_2^- which has been studied previously by negative ion photoelectron spectroscopy.[12,13] The photoelectron spectrum of SO_2^- is highly structured, showing a clear progression in ν_1, the symmetric stretching mode of SO_2, as well as less intense, but clearly resolved, transitions from vibrationally excited states of SO_2^-.

(1) Mead, R. D.; Stevens, A. E.; Lineberger, W. C. In *Gas Phase Ion Chemistry*; Bowers, M. T., Ed.; Academic: Orlando, 1984; Vol. III, Chapter 22.
(2) Drzaic, P. S.; Marks, J.; Brauman, J. I. In *Gas Phase Ion Chemistry*; Bowers, M. T., Ed.; Academic: Orlando, 1984; Vol. III, Chapter 21.
(3) Smyth, K. C.; Brauman, J. I. *J. Chem. Phys.* **1972**, *56*, 5993. EA(SeH) = 2.21 ± 0.03 eV.
(4) Compton, R. N.; Reinhardt, P. W.; Cooper, C. D. *J. Chem. Phys.* **1978**, *68*, 2023. $EA(SeF_6) = 2.9 \pm 0.2$ eV.
(5) Compton, R. N.; Cooper, C. D. *J. Chem. Phys.* **1973**, *59*, 4140. EA(TeF_6) = 3.34 eV.
(6) Page, F. M.; Goode, G. C. *Negative Ions and the Magnetron*; Wiley-Interscience: New York, 1974. EA(SeCN) = 2.64 eV.
(7) Coe, J. V.; Snodgrass, J. T.; Freidhoff, C. B.; McHugh, K. M.; Bowen, K. H. *J. Chem. Phys.* **1986**, *84*, 618.
(8) Freidhoff, C. B.; Coe, J. V.; Snodgrass, J. T.; McHugh, K. M.; Bowen, K. H. *Chem. Phys. Lett.* **1986**, *124*, 268.
(9) Freidhoff, C. B.; Snodgrass, J. T.; Coe, J. V.; McHugh, K. M.; Bowen, K. H. *J. Chem. Phys.* **1986**, *84*, 1051.
(10) Siegel, M. W.; Celotta, R. J.; Hall, J. L.; Levine, J.; Bennett, R. A. *Phys. Rev. A* **1972**, *6*, 607.
(11) Corderman, R. R.; Lineberger, W. C. *Annu. Rev. Phys. Chem.* **1978**, *30*, 347.
(12) Celotta, R. J.; Bennett, R. A.; Hall, J. L. *J. Chem. Phys.* **1974**, *60*, 1740.
(13) Nimlos, M. R.; Ellison, G. B. *J. Phys. Chem.* **1986**, *90*, 2574.

0022-3654/89/2093-1249$01.50/0

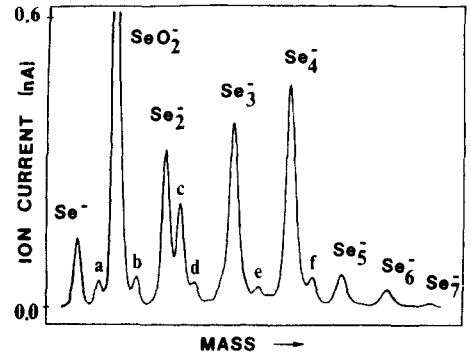

Figure 1. Mass spectrum showing the negative ions that are produced with hot elemental selenium and N_2O in a modified hot cathode discharge ion source. Peaks designated as a, b, c, d, e, and f refer respectively to the ions SeO^-, SeO_3^-, Se_2O^-, $Se_2O_2^-$, $Se_3O_2^-$, and $Se_4O_2^-$.

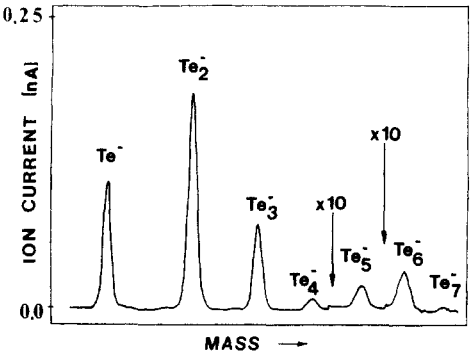

Figure 2. Mass spectrum showing the negative ions that are produced with hot elemental tellurium and Ar in a cold cathode Penning discharge ion source.

Transitions involving excitation in ν_3, the asymmetric stretch, are not expected or observed. Combination bands with n quanta of excitation in the ν_1 mode and 1 quantum in the ν_2 (bending) mode of SO_2 are also seen clearly in the photoelectron spectrum of SO_2^-. From this spectrum, the electron affinity of SO_2 has been determined to be 1.107 ± 0.008 eV.[13]

Our photoelectron spectrum of SeO_2^- presented in Figure 3 is qualitatively similiar to the SO_2^- photoelectron spectrum, and our interpretation of it is analogous. Peaks A, B, C, and D are separated from one another by about 920 cm^{-1}. This spacing is approximately equal to the symmetric stretching frequency of SeO_2 (922.6 cm^{-1}) in its ground electronic state.[14] Accordingly, these peaks are assigned as a progression in the symmetric stretching mode of the ground electronic state of SeO_2, these transitions having originated in the vibrational and electronic ground state of SeO_2^-.

The spacings between peaks D, E, and F are equal to about 810 cm^{-1}. We assign peaks E and F respectively as hot-band transitions from the (1,0,0) and (2,0,0) vibrational levels of ground-state SeO_2^- to the (0,0,0) level of ground-state SeO_2, where the notation (ν_1,ν_2,ν_3) indicates the degree of excitation in each vibrational mode. These assignments are supported by the observation that while the relative intensities of peaks A–D remained essentially constant with varying source conditions, the intensities of peaks E and F (relative to peaks A–D) changed considerably with ion source conditions. The observed spacings between peaks D, E, and F thus suggest that the symmetric stretching frequency for gas-phase SeO_2^- has a value of 810 ± 80 cm^{-1}. This is consistent with expectations based on the symmetric stretching frequencies of the related species, O_3 and O_3^- and SO_2 and SO_2^-, where in both cases the symmetric stretching frequency of the neutral is larger than that of the negative ion.

Although we do not observe distinct peaks that can be assigned as combination bands, a careful inspection of the photoelectron spectrum reveals that these features may well be present. The

(14) King, G. W.; McLean, P. R. *J. Mol. Spectrosc.* **1974**, *51*, 363.

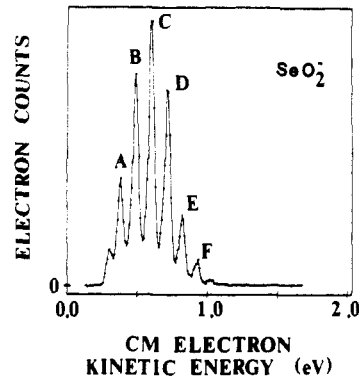

Figure 3. Photoelectron spectrum of SeO_2^-. This spectrum was recorded over about $^1/_2$ h with 2×10^{-9} A of SeO_2^- ion current and 150 circulating W of 2.540-eV photons.

features in the spectrum, which we have assigned as a vibrational progression in ν_1 (peaks A–D), consist of single vibronic transitions which have been broadened into peaks with a fwhm of ~55 meV by rotational and negative ion hot-band effects. This broadening obscures the areas between these peaks, which are the areas where combination bands are expected to appear. A close inspection of the shapes of these peaks near their bases shows distinct asymmetries, with additional intensity on their low electron kinetic energy sides. These low electron kinetic energy shoulders may be due both to negative ion hot-band transitions and to low-intensity combination bands. Although the relative contributions of these two effects are difficult to assess, the low intensities of the combination bands suggest similar bond angles in SeO_2 and SeO_2^-.

The electron affinity of SeO_2 can be calculated directly by subtracting the center-of-mass electron kinetic energy of peak D, assigned as the $SeO_2(0,0,0) \leftarrow SeO_2^-(0,0,0)$ transition, from the photon energy, giving a value of 1.823 ± 0.050 eV. In order to minimize the effects of SeO_2^- hot bands, this electron affinity value was not calculated from the SeO_2^- spectrum shown in Figure 3 but from another SeO_2^- spectrum in which the SeO_2^- vibrational temperature was significantly lower, as evidenced by greatly reduced intensities of peaks E and F. The uncertainty cited includes both the experimental uncertainty and the uncertainty in the exact location of the origin caused by rotational and remaining negative ion hot-band effects. Due to the scarcity of spectroscopic information on SeO_2^-, it is difficult to correct our electron affinity value for these effects, and we have chosen to leave it uncorrected and to incorporate this uncertainty into our error limits.

When a beam of TeO_2^- ions was crossed with a 2.540-eV photon beam, we found no evidence for photodetached electrons. Since our electron energy analyzer is sensitive to electrons with energies of ≥0.3 eV, we conclude that, unless TeO_2^- has an anomalously low photodetachment cross section, the electron affinity of TeO_2 must be >2.2 eV.

Se_2^- and Te_2^-. The homonuclear diatomic molecules of the group VIB elements O_2, S_2, Se_2, and Te_2 have similar electronic structures, and the photoelectron spectra of their negative ions are expected to reflect this similarity. However, several pertinent molecular properties change significantly between O_2 and Te_2. The lighter molecules are well-described by Hund's case "a" or "b" and have relatively small triplet splittings in their $^3\Sigma_g^-$ ground states. This splitting is characterized by $2\lambda_0$, where λ_0 is the spin coupling constant in the $v = 0$ vibrational level. For O_2, $2\lambda_0 \cong 4$ cm^{-1}, and for S_2, $2\lambda_0 \cong 24$ cm^{-1}.[15] As one proceeds to the heavier molecules, spin–orbit coupling becomes increasingly important, and the assumptions of Hund's case "c" become more appropriate. This results in the $^3\Sigma_g^-$ state splitting into a 0_g^+ ground state and a doublet 1_g state. The 1_g–0_g^+ splitting in Se_2 is 512 cm^{-1}, and in Te_2 it has increased to 1975 cm^{-1}.[16,17] In

(15) Huber, K. P.; Herzberg, G. *Molecular Spectra and Structure*; Van Nostrand Reinhold: New York, 1979; Vol. IV.

(16) Prosser, S. J.; Barrow, R. F.; Effantin, C.; d'Incan, J.; Verges, J. *J. Phys. B* **1982**, 4151.

TABLE I: Summary of Selected Spectroscopic Parameters for Group VIB Homonuclear Diatomic Molecules and Negative Ions[a]

molecule X_2	$EA(X_2)$, eV	$D_0(X_2)$, eV	$D_0(X_2^-)$, eV	$D_0(X_2)/D_0(X_2^-)$	$\omega(X_2)$, cm^{-1}	$\omega(X_2^-)$, cm^{-1}	$\omega(X_2)/\omega(X_2^-)$	triplet splitting in $X^3\Sigma_g^-(X_2)$, $2\lambda_0$, cm^{-1}	ref
O_2	0.440	5.116	4.09	1.25	1580	1090	1.45	4	15, 18
S_2	1.663	4.369	3.96	1.10	726	601	1.21	24	12, 15
Se_2	1.94	3.411[b]	3.33	1.02	385	330	1.17	512	15, 16, 31, pw
Te_2	1.92	2.625[c]	2.57	1.02	247			1975	17, pw

[a] pw = present work. [b] There remains some controversy over this value in the literature. We have chosen the spectroscopic value of 3.411 eV (ref 15) which agrees best with mass spectrometric values (ref 31). [c] We have chosen the most recent spectroscopic value of 2.625 eV (ref 17) which is a bit lower than the mass spectrometric value of 2.677 eV.

contrast to the increasing triplet splittings for the heavier diatomics, the fundamental vibrational frequencies $\omega_e(X_2)$ decrease from a value of 1580 cm^{-1} for O_2 to 247 cm^{-1} for Te_2. Bond dissociation energies $D_0(X_2)$ decrease from 5.1 eV for O_2 to 2.6 eV for Te_2. The electron affinities $EA(X_2)$, as we will show below, have been found to approach the electron affinities of their group VIB atoms EA(X) more and more closely as one proceeds down the VIB column of the periodic table to the heavier species. These properties are summarized in Table I.

The definitive determination of the electron affinity of molecular oxygen in 1972 was one of the earliest triumphs of negative ion photoelectron spectroscopy.[18] The photoelectron spectrum of O_2^- exhibits clearly defined vibrational progressions in both the ground ($X^3\Sigma_g^-$) and first excited ($a^1\Delta_g$) electronic states of O_2. An adiabatic electron affinity of 0.440 ± 0.008 eV for O_2 and an equilibrium bond length and rotational constant for O_2^- were obtained from an analysis of this spectrum. The small triplet splitting[15] in the $X^3\Sigma_g^-$ state of O_2 is completely unresolved at the ~0.050-eV resolution at which this spectrum was obtained. The photoelectron spectrum of S_2^- exhibits a single progression of peaks separated by the vibrational interval for the $X^3\Sigma_g^-$ state of neutral S_2.[12] Due to the higher electron affinity of S_2, the $a^1\Delta_g$ state was not energetically accessible with 2.540-eV photons. The small triplet splitting in the $X^3\Sigma_g^-$ state of S_2 remains completely unresolved. By interpreting the S_2^- spectrum in analogy with the O_2^- spectrum, the electron affinity of S_2 was determined to be 1.663 ± 0.040 eV. The larger uncertainty in the electron affinity of S_2 than in that of O_2 is due primarily to the lack of spectroscopic information available for S_2^-, which made correcting for rotational and fine structure effects infeasible.

In contrast to the situation in O_2 and S_2, where the triplet splittings are very small relative to vibrational frequencies, in Se_2 the triplet splitting is comparable to its 0.048-eV vibrational level spacing.[16] The splitting of the $X^3\Sigma_g^-$ state of Se_2 into a 0_g^+ ground state and a 1_g excited state 0.063 eV higher substantially complicates the expected Se_2^- photoelectron spectrum. Instead of a single vibrational progression, vibrational progressions to both states are expected, separated by the 0.063-eV 1_g–0_g^+ splitting in Se_2. The transitions to the 1_g state are expected to be twice as intense as those to the 0_g^+ state due to the relative degeneracies of these two states. However, because of the comparable magnitudes of the 1_g–0_g^+ splitting and the vibrational level spacing in Se_2, many of these transitions have nearly equal energies and will remain unresolved at our instrumental resolution of ~0.030 eV (fwhm).

Our photoelectron spectrum of Se_2^- is presented in Figure 4. Because of its many unresolved transitions, the spectrum was analyzed by comparing it with a modeled spectrum. The modeled spectrum's relative transition energies were calculated based on the 1_g–0_g^+ splitting in Se_2 and the vibrational spacings in Se_2 and Se_2^-.[15] Since its magnitude is unknown, no contribution from spin–orbit splitting effects in Se_2^- was included in the model. On the basis of the fact that the magnitude of this splitting in the isoelectronic neutral molecule, SeBr, is ~0.13 eV,[15] however, we do not expect an appreciable distortion of the Se_2^- spectrum due

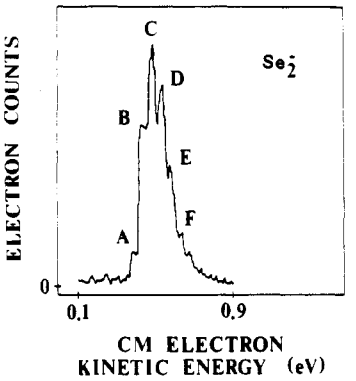

Figure 4. Photoelectron spectrum of Se_2^-. This spectrum was recorded over about $^1/_2$ h with 50 × 10^{-12} A of Se_2^- ion current and 150 circulating W of 2.540-eV photons.

TABLE II: Assignment of Se_2^- Photoelectron Spectrum[a]

peak	assignt	peak	assignt
A	$1_g(3,0)$	D	$1_g(0,0)$
			$0_g^+(1,0)$
B	$1_g(2,0)$		$0_g^+(2,1)$
	$0_g^+(3,0)$		$1_g(1,1)$
	$1_g(3,1)$		
		E	$0_g^+(0,0)$
C	$1_g(1,0)$		$1_g(0,1)$
	$0_g^+(2,0)$		$0_g^+(1,1)$
	$0_g^+(3,1)$		
	$1_g(2,1)$	F	$0_g^+(0,1)$
			$1_g(0,2)$

[a] The assignments are identified by using the notation $X(v',v'')$, where X indicates which Se_2 electronic state is the final state for the transition and v' and v'' indicate final and initial vibrational levels, respectively. All transitions listed originate in the Se_2^- electronic ground state.

to the population of its upper spin–orbit state. Transitions originating in the $v'' = 0$ and $v'' = 1$ levels of Se_2^- were included in the model. The relative transition intensities were determined by considering the degeneracies of the states involved and by assuming that the Franck–Condon factors for both manifolds were roughly equivalent to those in the analogous S_2^- photoelectron spectrum. Although this assumption is only an approximation, the conclusions drawn are not significantly changed due to substantial changes in the assumed Franck–Condon factors. The relative intensities of transitions originating in the $v'' = 0$ and $v'' = 1$ states of Se_2^- were chosen on the basis of Boltzmann populations for an ion source temperature of 700 K. After the relative transition energies and intensities were calculated, the modeled spectrum was generated by adding together all the transitions as Gaussian-shaped peaks with a fwhm of ~0.030 eV. Good agreement was found between the experimental and modeled spectrum when the $0_g(0,0)$ transition was assumed to be contained within peak E, where the notation used is $X(v',v'')$, with X indicating which Se_2 electronic state is the final state in the transition. The full assignment of the Se_2^- photoelectron spectrum is found in Table II. The modeling procedure yields a center-of-mass electron kinetic energy of 0.60 eV for the $0_g(0,0)$ transition, which leads to an electron affinity for Se_2 of 1.94 ± 0.07 eV. The error includes the uncertainty in the true $0_g(0,0)$ location due to

(17) Verges, J.; Effantin, C.; Babaky, O.; d'Incan, J. *Phys. Scr.* **1982**, *25*, 338.
(18) Celotta, R. J.; Bennett, R. A.; Hall, J. L.; Siegel, M. W.; Levine, J. *Phys. Rev. A* **1972**, *6*, 631.

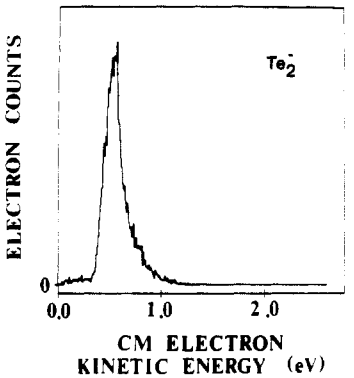

Figure 5. Photoelectron spectrum of Te_2^-. This spectrum was recorded over about 1 h with 30×10^{-12} A of Te_2^- ion current and 150 circulating W of 2.540-eV photons.

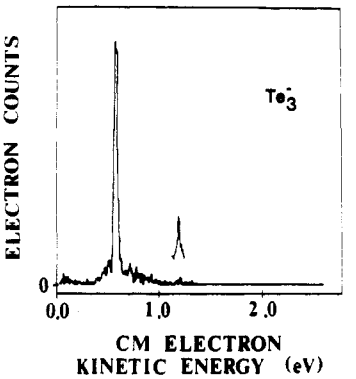

Figure 6. Photoelectron spectrum obtained when a beam of Te_3^- is crossed with a 2.540-eV photon beam. This spectrum was recorded over about 1 h with 30×10^{-12} A of Te_3^- ion current and 150 circulating W of 2.540-eV photons. The insert above the main spectrum is a limited range, long integration time scan from ~1.12 to 1.27 eV.

rotational effects and to Se_2^- hot-band effects. Previous estimates of EA(Se_2) are consistent with the value determined here.[19]

The Te_2 molecule has a 0.245-eV splitting between its $X0_g^+$ and $X1_g$ states and a 0.031-eV vibrational level spacing in both of these states.[17] Since this vibrational level spacing is nearly equal to the instrumental resolution and since the individual peaks will be somewhat broadened by rotational and Te_2^- hot-band effects, clearly resolved vibrational progressions are not expected in the Te_2^- photoelectron spectrum. Instead, the spectrum is expected to consist to two broad peaks spaced by approximately the 0.245-eV 1_g–0_g^+ splitting of Te_2, with each peak containing several closely spaced, unresolved vibronic transitions. The higher electron kinetic energy peak arises from transitions to the 0_g^+ state of Te_2 and, due to relative degeneracies, is expected to be half as intense as the lower electron kinetic energy peak which arises from transitions to the 1_g state of Te_2.

The 2.540-eV photoelectron spectrum of Te_2^- which we observe is presented in Figure 5. Only one peak is observed, and its fwhm is ~0.175 eV. We assign this feature as arising from transitions to the ground 0_g^+ state of Te_2 which originate in the lower vibrational levels of the ground electronic state of Te_2^-. If it were due to transitions to the upper 1_g state of Te_2, a second peak, half as intense at ~0.245 eV higher electron kinetic energy, would be expected. If present, this peak would be clearly visible in the photoelectron spectrum. Transitions to the 1_g state of Te_2 are not observed because the electrons photodetached as a result of these transitions possess kinetic energies that occur in a region of the spectrum where electron energy analyzers of necessity become increasingly insensitive. The high electron kinetic energy tail on the peak that we do observe is most likely due to transitions that originate in vibrationally excited states of Te_2^-. On the basis of previous work with the Penning source in which Te_2^- was generated, we suspect that the ion temperature is ~1000 K.[20] The $0_g^+(0,0)$ transition, which leads to the electron affinity of Te_2, is contained within the observed peak. Since the individual vibrational features are unresolved, a precise value for this transition energy is difficult to assign. The best value for the electron affinity of Te_2, which we have obtained by modeling the experimental spectrum using assumptions analogous to those employed in the Se_2^- case, is 1.92 ± 0.07 eV.

Se_3^- and Te_3^-. The ions O_3^- and S_3^- have both been studied previously by negative ion photoelectron spectroscopy. In both of these cases the negative ion photoelectron spectrum is highly structured, showing a clear progression in ν_1, the symmetric stretching mode of the neutral molecule. In addition, in the case of O_3^-, the photoelectron spectrum[21] contains a peak that arises from the photodissociation of O_3^- into $O_2 + O^-$ by the 2.540-eV photons, followed by photodetachment of the resulting O^-. In spite of the fact that this competing photodissociation channel is accessible, a O_3^- photoelectron spectrum is also clearly observed. The electron affinity of O_3, as determined by variable-frequency laser photodetachment,[21] is 2.1028 eV, in good agreement with the value obtained from the photoelectron spectrum. The photoelectron spectrum[13] of S_3^- shows no evidence for photodissociation. The electron affinity for S_3 determined from an analysis of its spectrum is 2.093 ± 0.025 eV. Knowing the electron affinity of S_3, one can calculate the bond dissociation energies for the dissociation reactions $S_3^- \rightarrow S_2^- + S$ and $S_3^- \rightarrow S^- + S_2$. These values are 3.27 and 2.87 eV, respectively. Since these are the minimum energies at which these photodissociation processes can occur, the absence of evidence for either process in the 2.540-eV photoelectron spectrum is reasonable. When we crossed a beam of Se_3^- ions with a 2.540-eV photon beam in our laboratory, we found no evidence for photodetachment or photodissociation. Thus, it appears that unless Se_3^- has an extraordinarily low photodetachment cross section, the electron affinity of Se_3^- must be greater than 2.2 eV.

The photoelectron spectrum we obtained when a beam of Te_3^- ions was irradiated with 2.540-eV photons is presented in Figure 6. The most prominent peak at ~0.6 eV in this spectrum occurs at the same electron kinetic energy as do the almost coincident $Te(^3P_2) \leftarrow Te^-(^2P_{3/2})$ and $Te(^3P_{0,1}) \leftarrow Te^-(^2P_{1/2})$ transitions in the photoelectron spectrum of atomic Te^-.[22] We attribute this peak to photodissociation of Te_3^- into Te_2 and Te^- predominantly in its $^2P_{3/2}$ ground state, followed by photodetachment of the resulting Te^- ions. The small peak at ~1.2 eV is due to the photodissociation of Te_3^- into Te_2 and Te^- in its $^2P_{1/2}$ excited state, followed by photodetachment of the resulting $Te^-(^2P_{1/2})$. By constructing a thermochemical cycle, we obtain the relation

$$\Delta H(1) = \mathrm{EA}(Te_3) + \mathrm{DH}(Te_2\text{–}Te) - \mathrm{EA}(Te) \qquad (2)$$

where $\Delta H(1)$ is the energy necessary for the dissociation of Te_3^- into $Te^-(^2P_{3/2})$ and Te_2, EA(Te_3) is the electron affinity of Te_3, DH(Te_2–Te) is the bond dissociation energy in Te_3, and EA(Te) is the electron affinity of Te. The prominent peak at ~0.6 eV in the spectrum implies an upper limit of 2.540 eV for $\Delta H(1)$. By estimating DH(Te_2–Te) from the atomization energy of Te_3[23] and the bond dissociation energy D_0 for Te_2[17] and knowing the electron affinity of Te from threshold photodetachment measurements,[22] one can calculate an upper limit of 2.7 eV for the electron affinity of Te_3 using eq 2. The observation of the smaller peak at ~1.2 eV suggests that the threshold for photodissociation of Te_3^- into $Te^-(^2P_{1/2})$ and Te_2 is less than 2.540 eV. If one assumes that all the Te_3^- ions in the beam are in their electronic, vibrational, and rotational ground states, the observation of this peak would lower the upper limit for the electron affinity of Te_3

(19) Christodoulides, A. A.; McCorkle, D. L.; Christophorou, L. G. In *Electron-Molecule Interactions and Their Applications*; Christophorou, L. G., Ed.; Academic: Orlando, 1984; Vol. 2, Chapter 6.
(20) Snodgrass, J. T.; Coe, J. V.; Freidhoff, C. B.; McHugh, K. M.; Bowen, K. H. *Chem. Phys. Lett.* **1986**, *122*, 352.
(21) Novick, S. E.; Engelking, P. C.; Jones, P. L.; Futrell, J. H.; Lineberger, W. C. *J. Chem. Phys.* **1979**, *70*, 2652.
(22) Slater, J.; Lineberger, W. C. *Phys. Rev. A* **1977**, *15*, 2277–82.
(23) Neubert, A. *High Temp. Sci.* **1978**, *10*, 261–7.

TABLE III: Heats of Formation[a] of Some Selenium- and Tellurium-Containing Gas-Phase Negative Ions (in kcal/mol)

ion	$\Delta H_f°_{298.15}$	ion	$\Delta H_f°_{298.15}$
Se_2^-	−11	TeO^-	−25
Te_2^-	−8	SeO_2^-	−69
SeO^-	−22		

[a] These heats of formation were calculated from eq 4, the electron affinities listed in Table V, and the heats of formation listed in ref 32–34. Typical uncertainties are ~±3 kcal/mol.

TABLE IV: Bond Dissociation Energies[a] of SeO_2^-, Se_2^-, and Te_2^- (in kcal/mol)

ion	products	$DH°_{298}$	ion	products	$DH°_{298}$
SeO_2^-	$SeO^- + O$	107	SeO^-	$Se^- + O$	88
SeO_2^-	$SeO + O^-$	106	SeO^-	$Se + O^-$	101
Se_2^-	$Se^- + Se$	72	TeO^-	$Te^- + O$	85
Te_2^-	$Te^- + Te$	55	TeO^-	$Te + O^-$	96

[a] These bond dissociation energies were calculated by using the heats of formation listed in Table III and ref 32–34. Typical uncertainties are ~±3 kcal/mol.

by the 0.62-eV energy difference between $Te^-(^2P_{1/2})$ and $Te^-(^2P_{3/2})$ to ~2.1 eV. The low intensity of this peak may suggest, however, that it is in fact due to the population of levels in the Te_3^- ions sufficiently energetic to make photodissociation of Te_3^- into $Te^-(^2P_{1/2})$ and Te_2 accessible with 2.540-eV photons. We, therefore, conservatively cite 2.7 eV as an upper limit for the electron affinity of Te_3.

The photoelectron intensity surrounding the base of the most prominent peak in the spectrum shown in Figure 6 occurs over the same energy range as the Te_2^- photoelectron spectrum shown in Figure 5. By constructing a thermochemical cycle for the photodissociation of Te_3^- into Te_2^- and ground-state Te, we obtain the relation

$$\Delta H(2) = EA(Te_3) + DH(Te_2\text{–}Te) - EA(Te_2) \quad (3)$$

where $\Delta H(2)$ is the energy necessary for the dissociation of Te_3^- into Te_2^- and $Te(^3P_2)$. Comparison of eq 2 and 3 shows that the difference in the energy required for the dissociation of Te_3^- into Te^- and Te_2 and the energy needed for the dissociation of Te_3^- into Te_2^- and Te is given by the difference in the electron affinities of Te and Te_2. We know from our work on Te_2^- described previously that this difference is small, ~0.05 eV. Thus, it is plausible that when Te_3^- ions are irradiated with 2.540-eV photons, some photodissociate to give Te_2^- and Te and that some of these nascent Te_2^- ions are then photodetached. It is also possible that part of the photoelectron intensity surrounding the peak at ~0.6 eV is due to photodetachment from Te_3^- ions that were not photodissociated. The fundamental vibrational frequencies of Te_3 are below our instrumental resolution,[24] and we would not expect a structured photoelectron spectrum. This possibility is, of course, also consistent with the upper limit we have placed on the electron affinity of Te_3.

Discussion

Heats of Formation and Bond Dissociation Energies. If we combine the electron affinities that we have determined with thermochemical data available in the literature, several previously unknown negative ion heats of formation and negative ion bond dissociation energies can be calculated. The heat of formation of a negative ion $\Delta H_f°_{298}$ (X^-) is given by

$$\Delta H_f°_{298}(X^-) = \Delta H_f°_{298}(X) - EA(X) - \int_{0K}^{298K} C_p(e^-)\, dT \quad (4)$$

The integrated heat capacity of the electron is taken as $^5/_2RT$ = 1.481 kcal/mol at 298.15 K.[25] We have chosen to include this term in order to make the values reported here compatible with those in the JANAF tables.[26] Negative ion heats of formation are listed in Table III. Several negative ion bond dissociation energies calculated by using these heats of formation are listed in Table IV.

TABLE V: Electron Affinities (eV) of Some Molecules Containing Group VIB Atoms[a]

	EA	ref		EA	ref
O	1.461	35	OH	1.828	36
S	2.077	1	SH	2.317	37
Se	2.021	1	SeH	2.21	3
Te	1.971	22	TeH	2.102	9
O_2	0.440	18	O_2	0.440	18
S_2	1.663	12	SO	1.126	38
Se_2	1.94	pw	SeO	1.456	7
Te_2	1.92	pw	TeO	1.697	8
O_3	2.103	21	O_3	2.103	21
S_3	2.093	13	SO_2	1.107	13
Se_3	>2.2	pw	SeO_2	1.823	pw
Te_3	≤2.7	pw	TeO_2	>2.2	pw

[a] pw = present work.

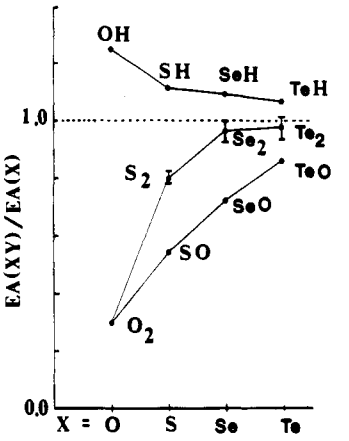

Figure 7. Electron affinity (EA) trends for the group VIB diatomic hydrides, homonuclear diatomics, and monoxides. X denotes the group VIB atoms O, S, Se, and Te. Y denotes H for the diatomic hydrides, X for the homonuclear diatomics, and O for the monoxides.

Electron Affinity Trends. Cotton and Wilkinson[27] have pointed out that, while there is a large difference between the chemical properties of oxygen and sulfur, the change in properties through the sequence sulfur, selenium, tellurium, and polonium is more gradual. This discontinuity in properties at oxygen has been attributed to the destabilization of the oxygen atom due to its small size. The small size of the oxygen atom results in its electronic charge being highly concentrated. This exerts a strong repulsive force upon any external electron that enters its outer shell, whether in forming a negative ion or covalent bond.[28] This interaction is reflected in the electron affinities of the group VIB atoms which increase gradually from polonium to sulfur, before decreasing dramatically at oxygen. (See Table V.) An analogous discontinuity at fluorine has been noted among the halogens.[29]

The electron affinities reported here, together with the electron affinities reported earlier for SeO, TeO, and TeH,[7-9] allow an examination of the systematic variations in the electron affinities of small molecules containing group VIB atoms. The data are most complete for the diatomic hydrides, homonuclear diatomics, and monoxides. The electron affinities of these categories of molecules all approach the electron affinities of their group VIB atoms more closely as one proceeds down the VIB column of the periodic table toward the heavier species. This result has been predicted for the diatomic hydrides by Cade.[30] These trends are

(24) Schnockel, H. *Anorg. Allg. Chem.* **1984**, *510*, 72–8.
(25) Lias, S. G. In *Kinetics of Ion-Molecule Reactions*; Ausloos, P., Ed.; Plenum: New York, 1979.
(26) Stull, D. R.; Prophet, H. *JANAF Thermochemical Tables*; U.S. Government Printing Office: Washington, D.C, 1971; NSRDS-NBS 37.
(27) Cotton, F. A.; Wilkinson, G. *Advanced Inorganic Chemistry*, 3rd ed.; Interscience: New York, 1972.
(28) Politzer, P. *Inorg. Chem.* **1977**, *16*, 3350.
(29) Politzer, P. *J. Am. Chem. Soc.* **1969**, *91*, 6235.

illustrated in Figure 7. In this figure and in the following discussion, X denotes the group VIB atoms O, S, Se, and Te. Y denotes H for the diatomic hydrides, X for the homonuclear diatomics, and O for the monoxides. Note the discontinuity between O and S in the ratio EA(XY)/EA(X) among the diatomic hydrides, and among the homonuclear diatomics, and the relatively smooth variation of this ratio among the monoxides. Insight into the significance of the trends illustrated in Figure 7 can be gained by considering the energetic relationships between the electron affinities of these molecules and the electron affinities of the group VIB atoms which they contain. A general relationship that applies to the diatomic hydrides, homonuclear diatomics, and monoxides is given by

$$EA(X) - EA(XY) = D_0(XY) - D_0(XY^-) \quad (5)$$

where $D_0(XY)$ and $D_0(XY^-)$ denote the bond dissociation energies of XY and XY^-. The decreasing differences between the electron affinities of X and XY through the sequence X = O, S, Se, and Te implies an increasing similarity between the bond dissociation energies of neutral XY and its negative ion XY^-. This increasing chemical similarity between the neutral molecules and their negative ions is perhaps due to the increasing diffuseness of the molecular orbitals in which the negative ions' excess electrons reside and the decreasing influence of such electrons on the bonding in these ions. For the homonuclear diatomics and monoxides, this suggestion is also supported by the fact that the vibrational frequencies of XY and XY^- become increasingly similar through the same sequence. Electron affinity trends among the triatomics and dioxides are more complicated and less clearly characterized.

Summary

By recording and analyzing the photoelectron spectra of SeO_2^-, Se_2^-, and Te_2^-, we have found the electron affinities of SeO_2, Se_2, and Te_2 to be 1.823 ± 0.050, 1.94 ± 0.07, and 1.92 ± 0.07 eV, respectively. We have also found the symmetric stretching frequency for SeO_2^- in its electronic ground state to be 810 ± 80 cm^{-1}. The ions TeO_2^- and Se_3^- do not photodetach electrons when irradiated with 2.540-eV photons, implying electron affinities for TeO_2 and Se_3 greater than 2.2 eV. Te_3^- has a propensity to photodissociate into Te^- and Te_2 and probably also into Te_2^- and Te when irradiated with 2.540-eV photons. These photodissociation processes imply an upper limit of ~2.7 eV for the electron affinity of Te_3. The electron affinities of the molecules X_2, XH, and XO, where X represents O, S, Se, and Te, are seen to become increasingly similar to the electron affinities of their group VIB atoms, X, through the sequence O, S, Se, and Te.

Acknowledgment. We thank Gary Posner for supplying us with SeO_2 powder during the initial experiments and Mike Bowen for supplying us with Te powder. This research was supported in part by the National Science Foundation under Grant CHE-8511320, the Research Corporation, and the Biomedical Research Support Grant Program, Division of Research Resources, National Institutes of Health (BRSG Grant S07 RR07041). Acknowledgment is also made to the donors of the Petroleum Research Fund, administered by the American Chemical Society, for partial support of this research.

Registry No. SeO_2, 7446-08-4; Se_2, 12185-17-0; Te_2, 10028-16-7; TeO_2, 7446-07-3; Se_3, 12597-24-9; Te_3, 50645-41-5.

(30) Cade, P. E. *Proc. Phys. Soc.* **1967**, *91*, 842–54.
(31) Drowart, J.; Smoes, S. *J. Chem. Soc., Faraday Trans. 2* **1977**, *73*, 1755.
(32) *CRC Handbook of Chemistry and Physics*, 66th ed.; CRC: Boca Raton, FL, 1985. All values in kcal/mol: $\Delta H_f°_{298}(Se) = 54.27$, $\Delta H_f°_{298}(Te) = 47.02$, $\Delta H_f°_{298}(Se_2) = 34.9$, $\Delta H_f°_{298}(SeO) = 12.75$, $\Delta H_f°_{298}(TeO) = 15.6$, $\Delta H_f°_{298}(O) = 59.553$.
(33) Barin, I.; Knacke, O.; Kubaschewski, O. *Thermochemical Properties of Inorganic Substances—1977 Supplement*; Springer-Verlag: Berlin, 1977. $\Delta H_f°_{298}(Te_2) = 38.03$ kcal/mol.
(34) Mills, K. C. *Thermodynamic Data for Inorganic Sulphides, Selenides and Tellurides*; Butterworths: London, 1974. $\Delta H_f°_{298}(SeO_2) = -25.8$ kcal/mol.
(35) Neumark, D. M.; Lykke, K. R.; Andersen, T.; Lineberger, W. C. *Phys. Rev. A* **1985**, *32*, 1890–2.
(36) Schulz, P. A.; Mead, R. D.; Jones, P. L.; Lineberger, W. C. *J. Chem. Phys.* **1982**, *77*, 1153.
(37) Breyer, F.; Frey, P.; Hotop, H. *Z. Phys. A* **1981**, *300*, 7.
(38) Lineberger, W. C. In *Laser Spectroscopy*; Brewer, R., Mooradian, A., Eds.; Plenum: New York, 1974; pp 581–95.